COMPUTATIONAL SIMULATION OF PULSATING TURBULENT FLOW IN PIPES

Fernando A. Ribas Junior
Federal University of Santa Catarina , Florianópolis, SC, 88040-900, Brazil
ribas@nrva.ufsc.br

César J. Deschamps
Federal University of Santa Catarina , Florianópolis, SC, 88040-900, Brazil
deschamps@nrva.ufsc.br

Abstract. The present work considers the numerical simulation of pulsating turbulent flow in pipes. This flow situation is found in several technological applications such as, for instance, compressors and I.C. engines. Therefore, a better understanding of this class of flow can provide important data to improve their performance. The conventional statistical approach for stationary turbulent flow is to decompose the instantaneous flow properties into a time-averaged component and a fluctuating component. Due to the non-stationary character of the flow considered here, an equivalent definition is required and is based on an ensemble averaging over a statistically acceptable number of cycles. The governing equations written for such ensemble-averaged properties are closed here using the concept of 'turbulent' or 'eddy' viscosity, which is evaluated with three different turbulence models: the k-ε model of Launder and Sharma (1974), the V2F model of Durbin (1991) and the k-ω model of Wilcox (1994). The equations are discretized and solved through the finite volume methodology. Friction factor, velocity profile and Reynolds stress are some of the analyzed variables. For a number of transient conditions, the V2F model has been shown to return the best agreement with experimental data. In some flow situations, a process of relaminarization has been found.

Keywords. *transient flow, pulsating flow, turbulence modeling, pipe flow.*

1. Introduction

The physical understanding of unsteady or periodic flows is a requirement in the development and optimization of several applications, such as compressors, I.C. engines, turbomachineries, etc. The fully developed periodic pipe flow in which the flow rate is forced to vary sinusoidally with time around a mean value represents one of the simplest flows under this category and, therefore, it is a natural choice for basic studies of unsteady flows.

One of the first works reported on pulsating flow is that of Uchida (1956), in which an analytical solution was obtained for a fully developed laminar pulsating flow through a pipe. Despite its relevance towards the understanding of the phenomenon, it should be noted that the turbulent flow regime prevails in virtually all technological applications. Since turbulence is not open to an analytical treatment, numerical modeling and experimental investigation are the only alternatives.

A number of experimental investigations have been done in the past 20 years considering pulsating fully developed turbulent flow in pipes (Ramaprian and Tu, 1983a; Ramaprian and Tu, 1983b; Mao and Hanratty, 1986; Finnicum and Hanratty, 1988; Barker and Williams, 2000). An important result from these works shows that shear stress at the wall varies out of phase in relation to the flow rate. The phase difference changes monotonically from the quasi steady value of zero degree to the quasi-laminar value of approximately 45 degrees at high frequencies. Another interesting result shows a departure of the velocity profile from the log law in wall regions. This is a critical aspect for turbulence modeling approaches that use wall functions to avoid solving the viscous sublayer region.

A relaminarization phenomenon has been observed when the flow undergoes a strong acceleration. This is associated with the confinement of the shear layer inside the viscous sublayer, causing the turbulence production to vanish. As a consequence, the flow can not maintain its turbulent regime and laminarizes even at high Reynolds number. The prediction of this flow feature is crucial in technological applications, since relaminarization reduces heat transfer and friction factor.

Ohmi et al. (1978), Kita et al. (1980), Ramaprian and Tu (1983a) and Mao and Hanratty (1986) showed that algebraic turbulence models cannot predict satisfactorily pulsating flows. This failure has been attributed to the absence of both transport equations for turbulence quantities and a transient term in their formulation. To circumvent this problem, Cotton and Ismael (1996) used a transport turbulence model, represented by the k-e model of Launder and Sharma (1974), obtaining a good agreement with experimental data in a wide range of situations.

The goal of the present work is to further investigate the turbulence modeling of pulsating turbulent flows. To that extent the k-ω model of Wilcox (1994) and the V2F model of Durbin (1991) have been selected. The quantities of interest are friction factor, wall shear stress, Reynolds stress, phase difference between flow rate and wall shear stress and velocity profile. The analysis should also indicate the more suitable model to predict this flow condition.

2. Turbulence Modeling

The flow is considered to be fully developed, turbulent, incompressible and undergoing a pulsating condition represented by a harmonically oscillation of the flow rate as follows:

$$U_m(t) = \overline{U}_m(1+\gamma\cos(\omega t)) \tag{1}$$

where $U_m(t)$ is the mean axial velocity varying with time t, $\overline{U_m}$ is the mean phase average axial flow velocity, γ is the amplitude of oscillation, ω is the radial velocity and t is the time.

The URANS (Unsteady Reynolds Average Navier Stokes equation) for the axial component of the momentum equation reads

$$\frac{\partial U}{\partial t} = -\frac{1}{\rho}\frac{dp}{dx} + \frac{1}{r}\frac{\partial}{\partial r}\left(r\left(\nu\frac{\partial U}{\partial r} - \overline{uv}\right)\right) \tag{2}$$

where U, dp/dx, and $-\overline{uv}$ are phase-averages for axial velocity, pressure gradient and Reynolds stress, respectively. It should be mentioned that U and $-\overline{uv}$ are functions of radial position and time, whereas the pressure gradient is a function of time only. The density ρ and the kinematic viscosity ν ($=\mu/\rho$) are considered to be constants.

The Reynolds stress, required to close Eq. (2), is modeled based on the eddy viscosity hypothesis, that is

$$-\overline{uv} = \nu_t\frac{\partial U}{\partial r} \tag{3}$$

where ν_t is the turbulence kinematic viscosity. Equations (2) and (3) are solved subject to the constraint that the average mean velocity at any instant t should satisfy the continuity equation expressed by Eq. (1). Therefore, Eq. (1) is used to correct the pressure gradient so that continuity is reached. The evaluation of the turbulence viscosity, ν_t, required to close the system of equations is carried out through three different turbulence models: i) the Low Reynolds Number k-ε model of Launder e Sharma (1974); ii) the k-ω model of Wilcox (1994) and iii) the V2F model of Durbin (1991).

The k-ε model and the k-ω model use damping functions to mimic the physical behavior in the proximity of walls. The V2F model is a three equation model and according to Durbin (1991) is capable of predicting the near wall region and highly anisotropic flows with accuracy. The model solves a differential equation for the Reynolds stress $\overline{v^2}$ normal to the streamline, which describes the near wall region better than the turbulence energy k because close to the wall turbulence is anisotropic, with $\overline{v^2}$ being the most affected stress by the wall proximity. More details on the V2F model can be found in Durbin (1991).

Since the k-ε model of Launder e Sharma (1974) is widely known, here only the transport equations for the k-ω model and for the V2F will be presented.

For the fully developed flow situation considered in this work, the k-ω model can be expressed as follows:

$$\frac{\partial k}{\partial t} = P + \frac{1}{r}\frac{\partial}{\partial r}\left(r\left(\nu + \frac{\nu_t}{\sigma_k}\right)\frac{\partial k}{\partial r}\right) - c_k f_k \omega k \tag{4}$$

$$\frac{\partial \omega}{\partial t} = c_{\omega 1} f_\omega \frac{\omega}{k}P - c_{\omega 2}\omega^2 + \frac{1}{r}\frac{\partial}{\partial r}\left(r\left(\nu + \frac{\nu_t}{\sigma_\omega}\right)\frac{\partial \omega}{\partial r}\right) \tag{5}$$

where,

$$\nu_t = c_\mu f_\mu \frac{k}{\omega} \;;\quad \text{where} \quad \omega = \frac{\varepsilon}{k} \tag{6}$$

$$P = \nu_t\left(\frac{\partial U}{\partial r}\right)^2 \tag{7}$$

The model constants are $c_\mu = 1.0$, $c_k = 0.09$, $c_{\omega 1} = 0.56$, $c_{\omega 2}=0.075$, $\sigma_k = \sigma_\omega = 2.0$. The model adopts the following damping functions

$$f_\mu = (0.025 + R_t/6.0)/(1.0 + R_t/6.0) \tag{8}$$

$$f_k = \left(0.278 + (R_t/8.0)^4\right)/\left(1.0 + (R_t/8.0)^4\right) \tag{9}$$

$$f_\omega = \left((0.1 + R_t/2.7)/(1.0 + R_t/2.7)\right) f_\mu^{-1} \tag{10}$$

where,

$$R_t = \frac{k^2}{\nu\varepsilon} \tag{11}$$

At the walls the non slip condition implies that k is equal to zero. Instead of prescribing ω at the wall, its value is evaluated for a volume adjacent to the wall according to $\omega = 6\nu/(c_{\omega 2} y^2)$, where **y** is the distance to the wall.

The V2F equations may be written as

$$\frac{\partial k}{\partial t} = P + \frac{1}{r}\frac{\partial}{\partial r}\left(r(\nu + \nu_t)\frac{\partial k}{\partial r}\right) - \varepsilon \tag{12}$$

$$\frac{\partial \varepsilon}{\partial t} = \frac{C'_{\varepsilon 1} P - C_{\varepsilon 2}\varepsilon}{T} + \frac{1}{r}\frac{\partial}{\partial r}\left(r\left(\nu + \frac{\nu_t}{\sigma_\varepsilon}\right)\frac{\partial \varepsilon}{\partial r}\right) \tag{13}$$

$$\frac{\partial \overline{v^2}}{\partial t} = kf - \frac{\overline{v^2}}{k}\varepsilon + \frac{1}{r}\frac{\partial}{\partial r}\left(r(\nu + \nu_t)\frac{\partial \overline{v^2}}{\partial r}\right) \tag{14}$$

$$f - L^2\left(\frac{\partial^2 f}{\partial r^2} + \frac{1}{r}\frac{\partial f}{\partial r}\right) = (C_1 - 1)\left(\frac{2/3 - \overline{v^2}/k}{T}\right) + C_2\frac{P}{k} \tag{15}$$

where,

$$\nu_t = C_\mu \overline{v^2} T \tag{16}$$

$$P = \nu_t\left(\frac{\partial U}{\partial r}\right)^2 \tag{17}$$

$$L = C_L \max\left(L'; C_\eta\left(\frac{\nu^3}{\varepsilon}\right)^{1/4}\right); \qquad \text{where} \qquad L' = \min\left(\frac{k^{3/2}}{\varepsilon}; \frac{1}{\sqrt{3}}\frac{k^{3/2}}{\overline{v^2} C_\mu \sqrt{P/\nu_t}}\right) \tag{18}$$

$$T = \min\left(T'; \frac{\alpha}{\sqrt{3}}\frac{k}{\overline{v^2} C_\mu \sqrt{P/\nu_t}}\right); \qquad \text{where} \qquad T' = \max\left(\frac{k}{\varepsilon}; 6\left(\frac{\nu}{\varepsilon}\right)^{1/2}\right) \tag{19}$$

The model constants are $C'_{\varepsilon 1} = 1.4\,(1 + 0.045\,[k/\overline{v^2}]^{1/2})$, C_μ= 0.22, C_L=0.25, C_η=85.0, α=0.6, C_1=1.4, C_2=0.3, $C_{\varepsilon 2}$=1.9, σ_ε=1.3.

At the walls *k* and $\overline{v^2}$ are set to zero, whereas the values for ε and f are set to the volume adjacent to the wall according to $\varepsilon = 2\nu k/y^2$ and $f = -20\nu^2 \overline{v^2}/(\varepsilon y^4)$, respectively, where **y** is the distance to the wall. The V2F equations, constant values and boundary conditions written here are based on the work of Manceau, et al.(2000) and Behnia et al.(1998).

3. Results

The first flow situation to be considered is that investigated by Ramaprian and Tu (1983a), in which water was pulsated through a pipe with a diameter of 50 mm. The authors have analyzed two flow situations: i) amplitude γ=0.64 and frequency f=0.5 Hz and ii) amplitude γ=0.15 and frequency f=3.6 Hz.

The results to be presented consider eight different angle positions in the cycle, with the deceleration period represented by the angles 0, 45, 90 and 135 degrees and the acceleration by the angles 180, 225, 270 and 315 degrees. Figures (1) and (2) show numerical and experimental results for Reynolds shear-stress distributions in the deceleration and the acceleration periods for the pulsating condition represented by γ=0.64 and f=0.5Hz. In order to assess the performance of the turbulence models, results for the V2F and the k-ω models are presented.

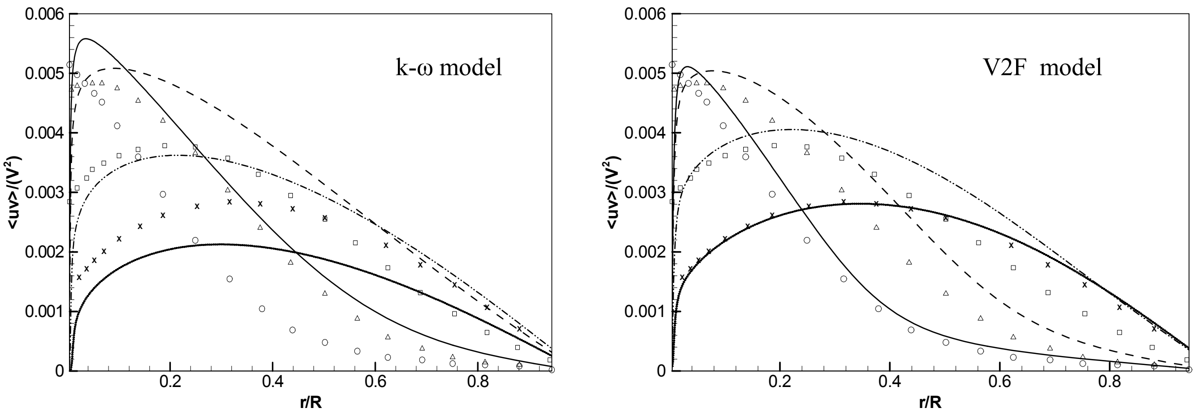

Figure 1. Numerical results compared to experimental data (Ramaprian and Tu, 1983a) for Reynolds-shear stress distributions with γ=0.64 and f=0.5 Hz. Deceleration period: O,———, $\theta=0^o$; Δ, — — — , $\theta=45^o$; □, — · · ., $\theta=90^o$; ×, ⋯⋯, $\theta=135^o$.

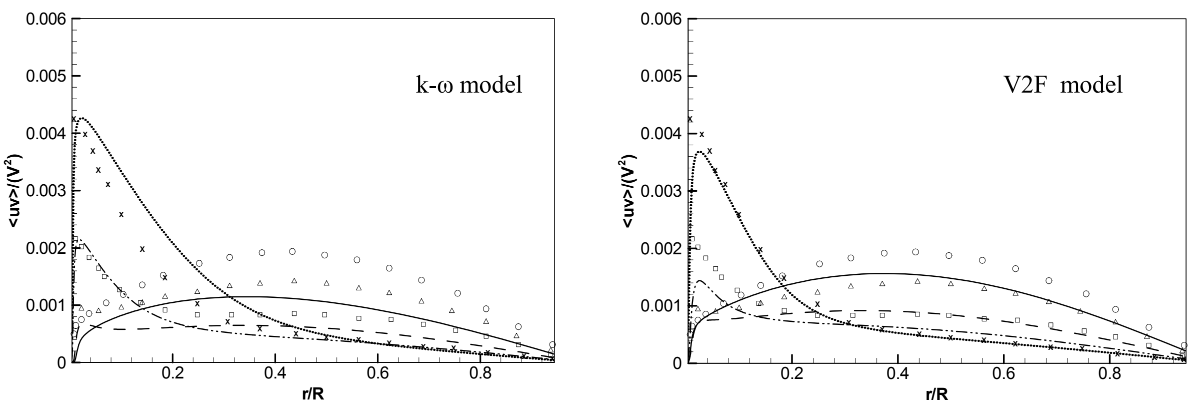

Figure 2. Reynolds-shear stress distributions and comparisons with experimental results (Ramaprian and Tu, 1983a) for γ=0.64 and f=0.5 Hz. Acceleration period: O,———,$\theta=180^o$; Δ, ———, $\theta=225^o$; □, —··, $\theta=270^o$; ×, ⋯⋯, $\theta=325^o$.

Figures (1) and (2) show that in general predictions returned by the V2F model are better than the those obtained with the k-ω model. Predictions obtained with the k-ε model are not shown here but in terms of accuracy are situated between the k-ω and the V2F models.

The explanation for the better agreement obtained with the V2F model can be attributed to the fact that it takes into account transients in the evaluation of turbulence scales. For instance, time and length scales in the near wall region are smaller than in the core region of the flow. In unsteady flow situations, this aspect plays an important role in the phenomenon, with each region responding in a different way to transients. Regions with greater time and length scales tend to respond more strongly than those with small time scales. The presence of a transport equation for the normal Reynolds stress $\overline{v^2}$ in the V2F means that length scales are evaluated taking into account transients.

It should be mentioned that the damping functions used in the k-ε and the k-ω models for the near wall region were not developed for unsteady problems, and their use are therefore questionable in transient situations.

Examining results in Fig. (1) and Fig. (2), one can clearly see a reduction in the levels of Reynolds stress in the acceleration period, which is likely associated to a process of relaminarization.

Turning attention to a flow situation with a higher frequency (γ=0.15 and f=3.6 Hz), Fig. (3) shows that the V2F model predicts a "frozen" structure for the Reynolds stress, which is not in line with the experimental data. The same behavior for turbulence has been also observed in the results given by the other models. This suggests that the eddy viscosity hypothesis is not adequate for such transients that other approaches must employed, such as Large Eddy Simulation.

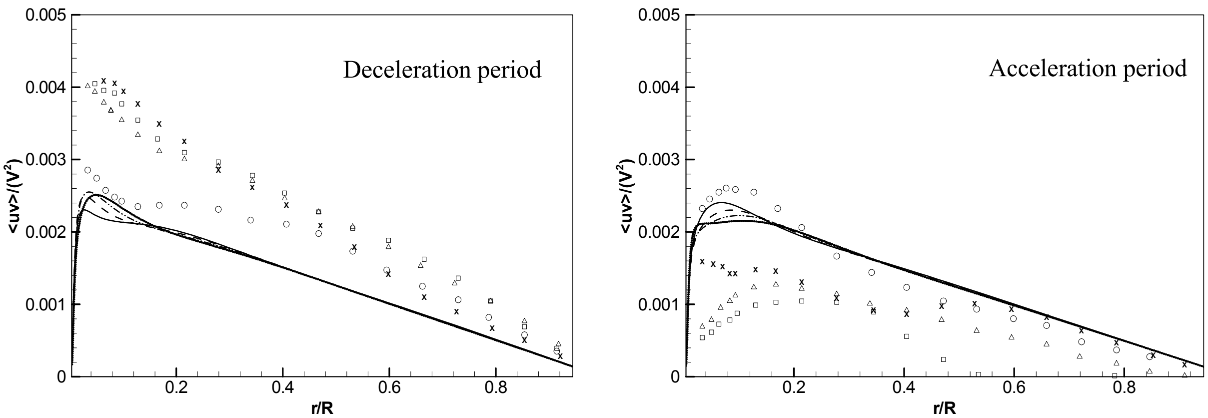

Figure 3. Numerical results (V2F model) and experimental data (Ramaprian and Tu, 1983) for Reynolds-shear stress distributions: γ=0.15 and f=3.6 Hz. Deceleration period: O,——,θ= 0^{o}; Δ, – – –, θ=45^{o}; □, –··, θ=90^{o}; $\times$, ······, θ=135^{o}. Acceleration period: O,——,θ= 180^{o}; Δ, – – –, θ=225^{o}; □, –··, θ=270^{o}; $\times$, ······, θ=325^{o}.

An interesting result that can be observed in Fig. (4), for γ=0.64 and f=0.5 Hz, is the departure of the velocity profile from the log law profile in the wall region, which is captured by the V2F model. This is a crucial aspect that has to be considered when using high Reynolds number turbulence models. This distortion in the velocity profile was not observed for the frequency f=3.6Hz investigated by Ramaprian and Tu (1983a).

It is possible to observe that the viscous sublayer is not affected by the pulsation. This can be attributed to the small turbulence scales, which makes the flow in this region to be statically independent of the transient imposed on the bulk flow. Naturally, one cannot discard a less physical explanation represented by the inability of the turbulence model to predict transient effects in the viscous sublayer. Figure (5) shows velocity profiles predicted by the k-ε for the same flow situation presented in Fig. (4). Results returned by the k-ω model do not show the level of agreement verified for the V2F and k-ε models.

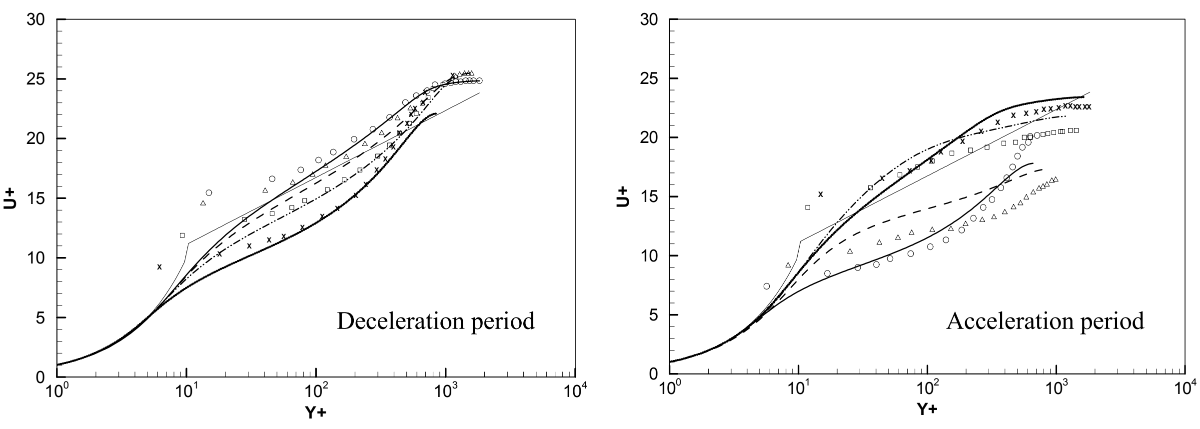

Figure 4. Numerical results (V2F model) and experimental data (Ramaprian and Tu, 1983a) for velocity profiles in the wall region: γ=0.64 and f=0.5 Hz. Deceleration period: log law, ——; O, ——,θ=0^{o}; Δ, – – –, θ=45^{o}; □, –··, θ=90^{o}; $\times$, ······, θ=135^{o}. Acceleration period: log law, ——; O, ——,θ=180^{o}; Δ, – – –, θ=225^{o}; □, –··, θ=270^{o}; $\times$, ······, θ=325^{o}.

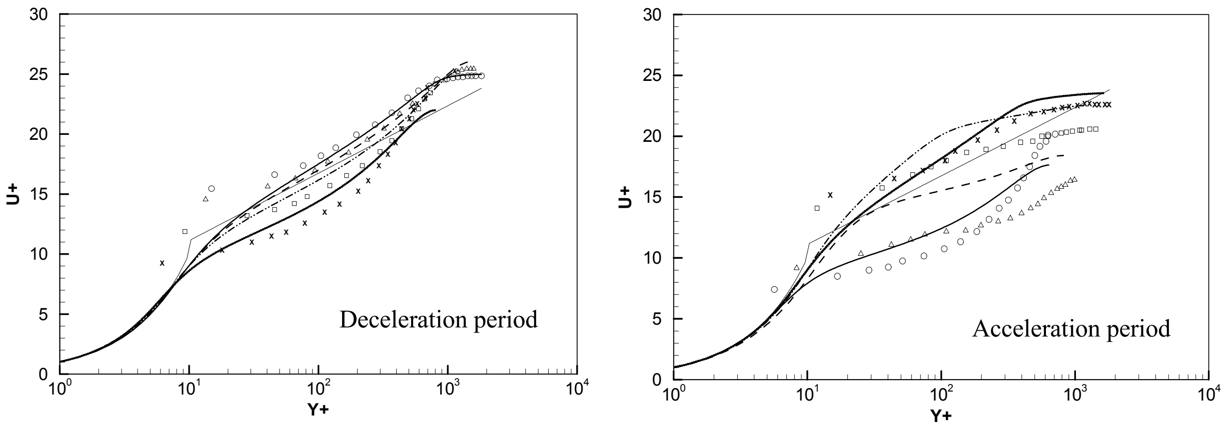

Figure 5. Numerical results (k-ε model) and experimental data (Ramaprian and Tu, 1983a) for velocity profiles in wall region: γ=0.64 and f=0.5 Hz. Deceleration period: log law, ——; O, ——,θ=0°; Δ, – – –, θ=45°; □, —··, θ=90°; × , ······, θ=135°. Acceleration period: log law, ——; O, ——,θ=180°; Δ, – – –, θ=225°; □, —··, θ=270°; ×, ······, θ=325°.

The friction factor f (=$\tau_w/\rho V^2$) is a parameter commonly adopted in the evaluation of engineering flow situations. Figure (6) shows predictions of friction factor for a pulsating flow, with γ = 0.2, f = 60 Hz and an average Reynolds number of 60,000. The results represent the ratio between the dynamic friction factor and the stationary friction factor, the latter calculated by the Blasius equation. For reference, the variation of the Reynolds number is also provided. As can be seen, the friction factor is strongly affected by the flow transient. This may be attributed to effects of inertia and of relaminarization in some parts of the period.

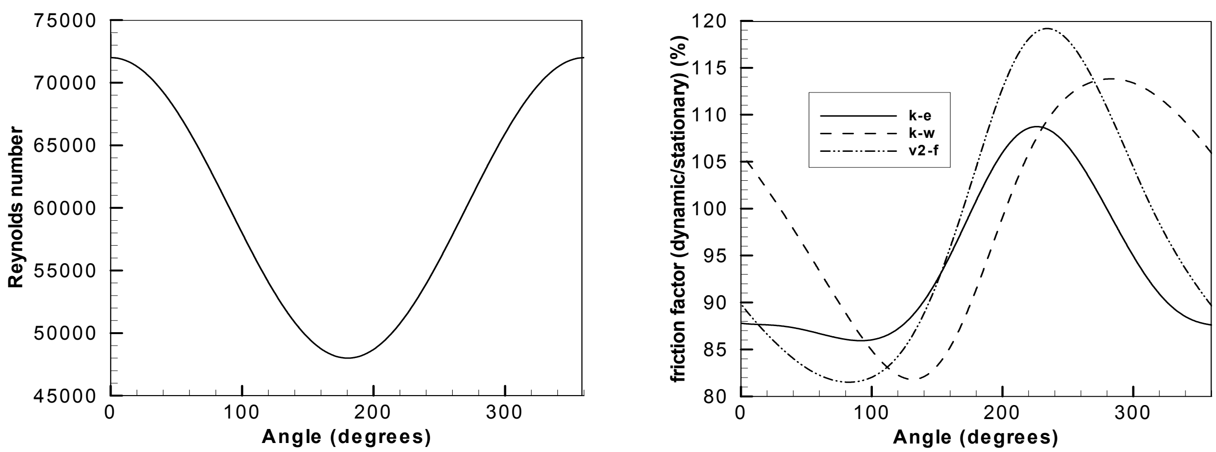

(a) Reynolds number (b) Friction factor

Figure 6. Numerical predictions for friction factor (Re_m = 60.000, γ = 0.2, f = 60 Hz).

4. Conclusions

Pulsating flow are found in many engineering applications and, therefore, a better understanding of its behavior can assist technological developments. In this work the k-ε model of Launder and Sharma (1974), the k-ω model of Wilcox (1994) and the V2F model of Durbin (1991) are employed to predict pulsating flows. The V2F model has been seen to return predictions that are in good agreement with experimental data. This is associated with its capability of taking into account transient terms in the evaluation of time and length scales.

Friction factor showed to be affected by flow transients and therefore this aspect should be considered in engineering calculations. Further tests in a wider range of amplitudes and frequencies are required to give a better assessment of this phenomenon. The analysis can be extended to the heat transfer problems since transients may affect also the Nusselt number (Barker and Williams, 2000).

5. References

Barker, A. R, Williams, J. E. F., 2000, "Transient measurements of the heat transfer coefficient in unsteady turbulent pipe flow", International Journal of Heat and Mass Transfer, Vol. 43, pp. 3197-3207.

Behnia, M., Parneix, S., Shabany, Y., Durbin, P. A., 1999, "Numerical study of turbulent heat transfer in confined and unconfined impinging jets", International Journal of Heat and Fluid Flow, Vol. 20, pp. 1-9.

Cotton, M. A, Ismael, J. O.,1996, "Calculations of wall shear stress in harmonically oscillated turbulent pipe flow using a low-Reynolds-number k-ε model", J. Fluid Eng., Vol. 118, pp. 189-194.

Durbin, P.A., 1991, "Near-wall turbulence closure modeling without "damping functions"". Theoret. Comput. Fluid. Dyn., No. 3, pp. 1-13.

Finnicum, D. S., Hanratty, T. J., 1988, "Influence of imposed flow oscillations on turbulence", PCH, Vol. 10, pp 585-598.

Ismael, J. O., Cotton, M. A., 1990, "Calculation of transient turbulent forced convection using a low-Reynolds-number k-ε model", Proc. 9th Int. Heat Transfer Conference.

Ismael, J.O., 1993, "Theoretical studies of unsteady turbulent pipe flow", Ph.D. thesis, University of Manchester.

Kita, Y., Adachi, Y., Hirose, K., 1980, "Periodically oscillating turbulent flow in a pipe", Bulletin of the JSME, Vol. 23, No. 179, pp. 656-664.

Launder, B. E., Sharma, B. I., 1974, "Application of the energy dissipation model of turbulence to the calculation of flow near a spinning disc", Letters in Heat and Mass Transfer, Vol. 1, pp. 131-138.

Mao, Z. X., Hanratty, T., 1986,, "Studies of the wall shear stress in a turbulent pulsating pipe flow", J. Fluid. Mech., Vol. 170, pp. 545-564.

Manceau, R., Parneix, S., Laurence, D., 2000, "Turbulent heat transfer predictions using V2F model on unstructured meshes", International Journal of Heat and Fluid Flow, Vol. 21, pp. 320-328.

Ohmi, M., Kyomen, S., Usui, T., 1978, "Analysis of velocity distribution in pulsating turbulent pipe flow with time-dependent friction velocity", Bulletin of the JSME., Vol. 21, No. 157, pp. 1137-1143.

Ramaprian, B. R., Tu, S. W., 1983a, "Fully developed periodic turbulent pipe flow. Part 1. Main experimental results and comparison with predictions", J. Fluid Mech., Vol. 137, pp. 31-58.

Ramaprian, B. R., Tu, S. W., 1983b, "Fully developed periodic turbulent pipe flow. Part 2. The detailed structure of the flow", J. Fluid Mech., Vol. 137, pp. 59-81.

Uchida, S., 1956, "The pulsating viscous flow superposed on the steady laminar motion of incompressible fluid in a circular pipe", ZAMP, Vol. 10, pp. 403-422.

Wilcox, D. C., 1994, "Turbulence Modeling for CFD", DCW Industries.